

GA-LDV: A Promising Derivative of 18 β -Glycyrrhetic Acid with Enhanced *in vitro* and *in vivo* Anti-Cancer Properties

Jiaying Zheng^{1,*}, Qiqi Feng^{1,*}, Qi Gao¹, Yaonan Wang¹, Shurui Zhao¹, Xiaoyi Zhang¹, Ming Zhao^{1,2}

¹Beijing Area Major Laboratory of Peptide and Small Molecular Drugs, Department of Medicinal Chemistry, School of Pharmaceutical Sciences, Capital Medical University, Beijing, 100069, People's Republic of China; ²Beijing Laboratory of Biomedical Materials and Key Laboratory of Biomedical Materials of Natural Macromolecules, Department of Biomaterials, College of Materials Science and Engineering, Beijing University of Chemical Technology, Beijing, 100026, People's Republic of China

*These authors contributed equally to this work

Correspondence: Ming Zhao, Department of Medicinal Chemistry, School of Pharmaceutical Sciences, Capital Medical University, Beijing, 100069, People's Republic of China, Tel +861083911535, Fax +861083911533, Email maozhao@126.com; Xiaoyi Zhang, Department of Medicinal Chemistry, School of Pharmaceutical Sciences, Capital Medical University, No. 10, Youanmenwaixitoutiao, Fengtai District, Beijing, 100069, People's Republic of China, Tel +861083911530, Fax +861083911533, Email zhangdd@ccmu.edu.cn

Purpose: The clinical translation of 18 β -Glycyrrhetic acid (GA) is impeded by its relatively low antitumor potency and poor aqueous solubility, we developed a novel derivative of GA by incorporating the Leu-Asp-Val (LDV) tripeptide to enhance its anti-tumor and anti-metastatic activities both *in vitro* and *in vivo*, thereby increasing its potential as a therapeutic agent for cancer treatment.

Methods: The water solubility of GA-LDV was evaluated. The inhibitory effects of GA-LDV on cell viability were assessed in four different human cancer cell lines. *In vitro* assays were conducted to measure the compound's impact on tumor cell adhesion, migration, and invasion. *In vivo* studies were performed using S180 and LLC xenograft models to evaluate the tumor inhibition and anti-metastatic properties.

Results: GA-LDV water solubility was increased 4.1 folds compared with GA. *In vitro* assays suggested that GA-LDV, at a concentration of 25 μ M, significantly impeded the adhesion, migration, and invasion of LLC tumor cell lines, with inhibition rates of 52.7%, 55.5% (vs GA 16.9%, $P < 0.05$) and 35.9% (vs GA 27.5%, $P < 0.05$). Moreover, GA-LDV demonstrated stronger tumor inhibition ability than GA ($P < 0.05$), and anti-metastasis activities in a dose-dependent manner, at the concentration of 5 μ mol/kg/d, 1 μ mol/kg/d, 0.2 μ mol/kg/d with lung metastatic nodules 7.5 ($P < 0.01$ compared with the control group), 9.8 ($P < 0.05$ compared with the control group) and 14.5. And GA-LDV had almost no systemic toxicity in S180 or LLC xenograft models.

Conclusion: The newly synthesized GA-LDV derivative demonstrates superior water solubility and significantly enhanced anti-tumor and anti-metastatic activities. The *in vitro* and *in vivo* studies indicate that GA-LDV is a promising candidate for further development as a cancer therapeutic agent, with the benefit of potentially reduced systemic toxicity.

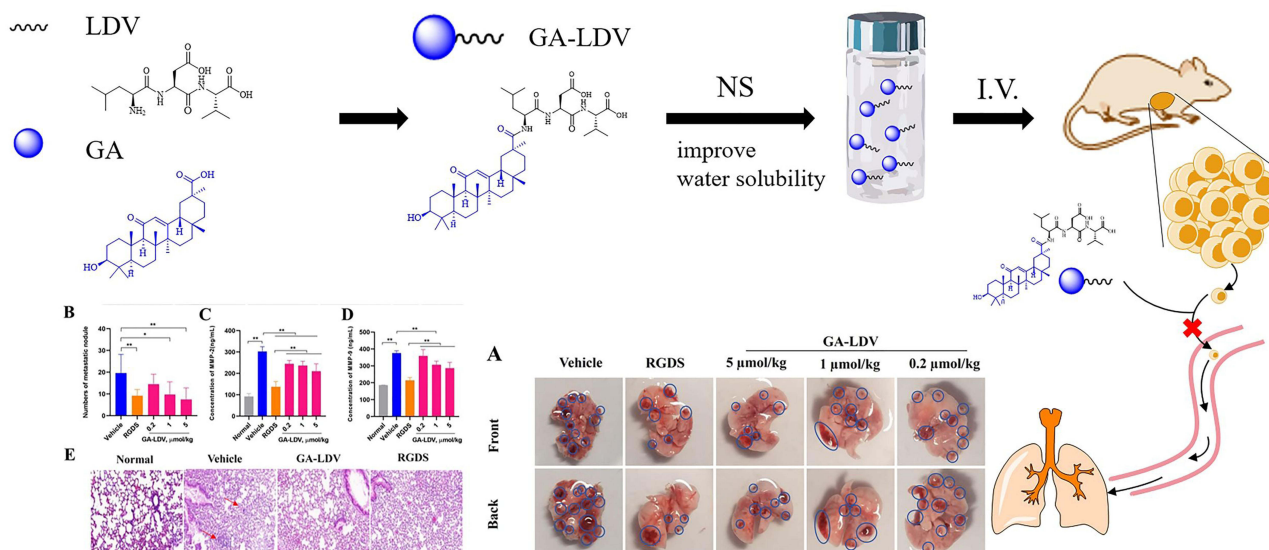
Keywords: 18 β -Glycyrrhetic acid, anti-tumor, anti-metastasis activity, lung cancer, MMP

Introduction

Malignant tumors pose a significant threat to human health, with approximately 90% of cancer-related mortalities attributed to tumor metastasis.^{1,2} Tumor metastasis is a multistep process that involves the shedding and invasion of tumor cells into local tissues, their entry into blood vessels or lymphatic vessels through degradation of the extracellular matrix, and their transfer with systemic circulation to a new anchorage point, where they adhere, invade, and migrate to new local tissues to form metastatic tumors.^{3,4} Matrix metalloproteinases (MMPs), especially MMP-2 and MMP-9, have important roles in promoting cancer metastasis and invasion.^{5,6} These proteases are key factors in the degradation of the extracellular matrix and have become important targets for anticancer drug development, promising for the treatment of metastatic malignant tumors.



Graphical Abstract



$\alpha 4\beta 1$ integrin is expressed in various cancers, including multiple myeloma, ovarian cancer, and pancreatic cancer, and recent studies have described its potential role in cancer progression and metastasis formation.^{7–10} Fibronectin (FN), an extracellular matrix protein, is known to interact with $\alpha 4\beta 1$ integrin through a specific tripeptide sequence, Leu-Asp-Val (LDV), which is located within the alternatively spliced connecting segment 1 (CS-1) domain.^{11,12} This interaction is crucial for the integrin's function in promoting cell adhesion, migration, and invasion—hallmarks of the metastatic cascade. Given the established link between $\alpha 4\beta 1$ integrin and tumor biology, therapeutic strategies that target this receptor could offer a novel avenue for the management of both primary tumors and metastatic disease.¹³ 18 β -Glycyrrhetic acid (GA) is an active molecule discovered from licorice root, which possesses a variety of pharmacological activities, notably its anti-tumor and anti-metastasis effects.¹⁴ GA has demonstrated the capacity to suppress the invasive and metastatic behavior of various cancer cells in both in vitro and in vivo, and the action that is often associated with the downregulation of matrix metalloproteinase (MMP) expression.^{15,16} Despite these promising biological activities, the clinical translation of GA is impeded by its relatively low antitumor potency and poor aqueous solubility, which can affect its bioavailability and therapeutic efficacy.^{17–19}

To overcome the identified limitations, we undertook the innovative design and synthesis of a novel GA derivative, GA-LDV. This novel compound was synthesized by conjugating the oligopeptide fragment Leu-Asp-Val (LDV) to the carboxyl terminus of GA. The selection of the LDV sequence, which is recognized for its high affinity to $\alpha 4\beta 1$ integrin, was strategic to augment the anti-cancer efficacy of GA. Our innovative derivative underwent a thorough evaluation of its anti-tumor and anti-metastatic capabilities, encompassing both in vitro and in vivo studies. Additionally, we delved into the underlying mechanisms, placing particular emphasis on the modulation of MMP expression and activity, which are pivotal for the metastatic process.

Materials and Methods

Solubility Determination

UV-spectrophotometer was used to measure the aqueous solubility of GA and GA-LDV with Lambert Beer law.²⁰ The maximum absorption wavelength (λ_{max}) of GA and GA-LDV in water was scanned in the UV range (200–400 nm). Different standard solutions of GA (3, 6, 9, 12, and 15 $\mu\text{g/mL}$) and GA-LDV (10, 20, 30, 40, and 50 $\mu\text{g/mL}$) were scanned on a spectrophotometer in the UV range 200–400 nm. The spectrum was recorded at 357 nm. The calibration

plot was constructed as concentration vs amplitude to draw the standard curve. Added 1 mg of the target compound to 1 mL of distilled water by Ultrasonic oscillation for 30 minutes, centrifuged at 10,000 r/min for 10 minutes. The supernatant was the saturated aqueous solution diluted 5 times to prepare the sample solution. The absorbance of GA and GA-LDV sample solutions was measured by UV-spectrophotometry, respectively. The concentration of the sample solution multiplied by 5 times equaled the saturation solution solubility.

Cell Cultures

All the cell lines (Human alveolar basal epithelial cell line A549, Human breast cancer cell line MCF-7, Human liver cancer cell line HepG-2, Mouse sarcoma cell line S180, Mouse lung cancer cell line LLC), Dulbecco's Modified Eagle Medium (DMEM), RPMI-1640 Medium and fetal bovine serum (FBS) were all purchased from Jiangsu KeyGEN BioTECH Corp. A549 was cultured in RPMI 1640, and LLC, HepG-2, S180, MCF-7 were cultured in DEME, with 10% PBS and 1% penicillin/streptomycin solution (100 U/mL penicillin and 100 µg/mL streptomycin), respectively. All the cell lines were grown in humidified 5% CO₂ atmosphere at 37°C.

Cell Proliferation and Viability Assay

Cell proliferation viability assay was measured by using the Cell Counting Kit-8 (CCK-8 kit).²¹ In brief, A549, HepG-2, MCF-7, LLC, S180 cells were plated at 5×10^4 cells per well in 96-well plates, allowed to recover for 4 hours before exposing to serial concentrations of GA and GA-LDV for 48 hours. 10 µL of CCK-8 solution was added and incubated for another 4 hours at 37°C and Optical Density (OD) was measured at 450 nm with a microplate reader.

Cell Adhesion Assay

To evaluate the adhesion properties of cancer cells to ECM proteins, a 96-well Nunc Maxisorp flat-bottom plate (Invitrogen) was coated overnight at 4°C using 10 µg/well fibronectin (BD BioCoat™). The plates were first washed with serum-free RPMI-1640 medium and 0.1% (w/v) BSA to remove unbound proteins, then blocked with serum-free RPMI-1640 medium and 0.5% (w/v) BSA for 1 hour at 37°C. 100 µL/well LLC cell suspension (5×10^5 /mL) treated with GA (25 µM), GA-LDV (25 µM) and RGDS (25 µM) were seeded in each well in triplicates and incubated for 1 hour at 37°C. Then, the non-adherent cells were washed off with PBS. Adherent cells were fixed with 4% paraformaldehyde solution for 15 min, images were acquired using by light microscope at $\times 200$ from 9 visual fields, and the number of adherent cells was analyzed using ImageJ software.

Cell Invasion Assay

A Transwell assay was performed to assess cell invasion capability.²² The 24-well BioCoat cell culture inserts (BD Biosciences, Bedford, MA, USA) with a polyethylene terephthalate membrane (8-µm porosity) were used, in which the membranes of the upper chamber were coated with Matrigel (1mg/mL, BD) and then incubated for 6 h at 37°C. The LLC cell suspension (5×10^6 /mL) treated with GA (25 µM), GA-LDV (25 µM) and RGDS (25 µM) was added into the upper chamber in serum-free media, and 0.6 mL complete culture medium was added into the lower chamber. After incubation for 7 h, the cells were washed twice with PBS, the remaining cells were wiped away using cotton swabs. 4% Paraformaldehyde was used as a fixation solution, and 0.1% crystal violet was used to stain. The number of invasion cells on the bottom surface of the membrane was counted under a light microscope at $\times 200$ from 9 visual fields. Experiments were performed 3 times in triplicate.

Cell Migration Assay

For the cell migration assay,²² Transwell membranes (8 µm pore size, 6.5 mm diameter, Corning Costar Corporation, Cambridge, MA) were used. 100 µL LLC cell suspension (5×10^6 /mL) treated with GA (25 µM), GA-LDV (25 µM) and RGDS (25 µM) were collected, washed, and re-suspended in serum-free medium in the upper chambers, while the lower chamber wells contained complete culture medium. After incubation for 7 h, the cells remaining on the upper membrane were carefully removed with cotton swap, while the migrated cells in the membrane of the lower chamber were fixed with 95% ethanol and stained with 0.1% crystal violet. The number of migration cells on the bottom surface of the membrane was counted under a light microscope at $\times 200$ from 9 visual fields. Experiments were performed 3 times in triplicate.

In vivo Antitumor of S180 Sarcoma

5-weeks old ICR male mice weighing 20.0 ± 2.0 g were purchased from Beijing Vital River Laboratory Animal Technology Co., Ltd. They were housed at $23 \pm 1^\circ\text{C}$ under 12h light/12h dark conditions with ad libitum access to food and water. All animal experiments were performed following relevant guidelines and regulations approved by the Experimental Animal Research Committee of Capital Medical University. The committee assured that the animal welfare was maintained in accordance with the requirements of Use of Laboratory Animals, and the ethics number is AEEI-2019-179. According to standard xenograft tumor research protocols,²³ mice were given subcutaneous injections of 1.5×10^6 sarcoma 180 (S180) cells in the exponential growth phase into the right axillary fossa on day 0. On day 5, mice were randomly divided into Vehicle (5% CMC-Na), Doxorubicin (Dox, $2 \mu\text{mol/kg/d}$), GA ($5 \mu\text{mol/kg/d}$) and GA-LDV ($5 \mu\text{mol/kg/d}$) group. All mice were administered intraperitoneally once a day for 10 days. After the experiment was completed, the mice were sacrificed and the tumors were removed and weighed. Inhibition of tumor growth was evaluated using percent inhibition relative to tumor weights in control tumor-bearing mice. Serum was collected for the ELISA experiments. The mice's organs (heart, liver, spleen, lung, kidney, brain) were obtained and embedded in paraffin for H&E staining.

In vivo LLC Sarcoma Metastasis Assay

Eight-week-old male C57BL/6 mice were purchased from Beijing Vital River Laboratory Animal Technology Co., Ltd. They were housed at $23 \pm 1^\circ\text{C}$ under 12h light/12h dark conditions with ad libitum access to food and water. All animal experiments were performed following relevant guidelines and regulations approved by the Experimental Animal Research Committee of Capital Medical University. The committee assured that the animal welfare was maintained in accordance with the requirements of Use of Laboratory Animals, and the ethics number is AEEI-2019-179. According to standard xenograft tumor research protocols,²⁴ 2×10^7 viable LLC cells were suspended in 0.2 mL of NS. This suspension was injected into the skin of the right armpit of C57BL/6 mice to form subcutaneous solid tumors. Ten days after injection, the tumor volume reached $\sim 50 \text{ mm}^3$ and the mice were randomly divided into Vehicle (5% CMC-Na), RGDS ($20 \mu\text{mol/kg/d}$), and GA-LDV (0.2, 1, $5 \mu\text{mol/kg/d}$) group. All mice were administered intraperitoneally once a day for 10 days. After the experiment was completed, the mice were sacrificed, and the tumors and lung were removed. The tumor tissue was weighed to represent the anti-tumor activity. The lung was used to count the metastasis nodule. Serum was collected for the ELISA experiments.

Serum MMP-2 and MMP-9 Determination

Mouse total MMP-2 ELISA kit (Shanghai Xitang Biotechnology Company, China) and mouse total MMP-9 ELISA kit (Shanghai Xitang Biotechnology Company, China) were used for quantitative detection of MMP-2 and MMP-9 in serum of S180-bearing mice and LLC sarcoma implanted C57BL/6 mice according to the manufacturer's instructions.

H&E Staining of Tissues

The hearts, livers, spleens, kidneys, brains of S180-bearing mice and the lungs of LLC sarcoma implanted C57BL/6 mice were fixed in a 10% neutral buffered formalin solution for 24 hours. After embedding in paraffin, 4-mm sections were prepared and stained with hematoxylin and eosin for microscopic observation.

TUNEL Stain

Terminal transferase-mediated dUTP nick-end labeling (TUNEL) staining of nuclear DNA in S180 tumor tissue cells was performed according to the manufacturer's instructions (Roche, USA). The fluorescence signals of different tissues were detected through fluorescence microscopy.

Statistical Analysis

All experiments were performed at least three times and all assays were repeated in triplicate. In the table or figure legends, the letter "n" represented the number of repeated experiments.

All the data was presented as mean \pm standard deviation (SD). The statistical analysis was performed with GraphPad Prism 8.0 and SPSS Version 21. Statistical significance was determined by one-way ANOVA. $P < 0.05$ was considered statistically significant.

Results

Synthesis of GA-LDV

As shown in [Supporting Information](#), we designed and synthesized GA-LDV by conjugating the oligopeptide fragment Leu-Asp-Val (LDV) to the carboxyl terminus of GA. The compound GA-LDV was structurally characterized using ^1H NMR ([Figure S1](#)), ^{13}C NMR ([Figure S2](#)), and MS ([Figure S3](#)).

Solubility Determination

The spectroscopic analysis revealed that both 18 β -Glycyrrhetic acid (GA) and its derivative GA-LDV exhibit a maximum absorption wavelength (λ_{max}) of 357 nm when dissolved in water. The calibration curves, derived from linear regression analysis, demonstrated a robust linear relationship within the concentration ranges of 3–15 $\mu\text{g}/\text{mL}$ for GA and 10–50 $\mu\text{g}/\text{mL}$ for GA-LDV. The corresponding linear regression equations for GA and GA-LDV were determined to be $Y = 0.01060X + 0.02960$ ($r^2 = 0.9928$) and $Y = 0.005590X + 0.007900$ ($r^2 = 0.9978$), respectively. The solubility of the saturated aqueous solutions of GA and GA-LDV was ascertained using established standard curves ([Figure 1A](#)), yielding solubility values of 39 $\mu\text{g}/\text{mL}$ for GA and 161 $\mu\text{g}/\text{mL}$ for GA-LDV ([Figure 1B](#)). These results demonstrate that the saturated aqueous solubility of GA-LDV is markedly higher (4.13-fold) than that of GA, underscoring its significance as a key parameter for potential pharmaceutical applications.

GA-LDV Inhibits the Proliferation of Cancer Cells

To determine the cytotoxic effects of GA-LDV, five cancer cell lines (A549, MCF-7, HepG2, S180, LLC) were treated with 100 μM GA or GA-LDV, and the CCK-8 assay determined the cell viability. As shown in [Table 1](#), both GA and GA-LDV had potent inhibitory effects on cancer cell proliferation in vitro, and there was no significant difference between the inhibitory activity of GA-LDV and GA. This finding suggests that the introduction of the LDV oligopeptide fragment does not compromise the cytotoxic potential of GA against the tested cancer cells, which is a pivotal consideration in the development of novel therapeutic agents.

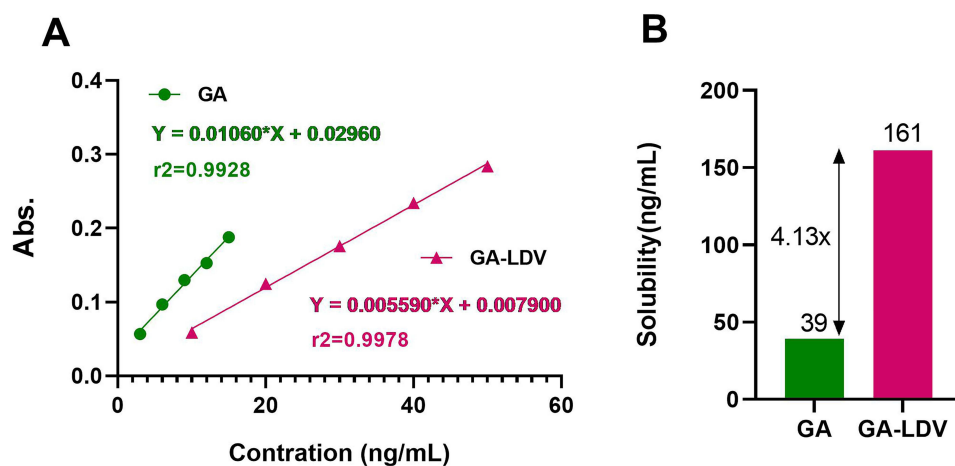


Figure 1 Standard curves of GA and GA-LDV aqueous solution (**A**) and solubility results (**B**).
Abbreviations: GA, 18 β -glycyrrhetic acid; GA-LDV, GA-Leu-Asp-Val.

Table 1 The Inhibition Rate (%) of 100 μ M GA and GA-LDV by the CCK-8 Assay

	A549	MCF-7	HepG2	S180	LLC
GA	59.5 \pm 2.4	19.5 \pm 13.8	35.1 \pm 7.2	21.2 \pm 4.8	23.4 \pm 7.9
GA-LDV	49.7 \pm 4.0	14.1 \pm 13.5	26.4 \pm 5.1	19.4 \pm 6.6	15.5 \pm 4.0

Notes: Inhibition rate = [(O.D of control group – O.D of treatment group)/O.D of control group] \times 100% (n = 6). Data were expressed as mean \pm SD.

Abbreviations: CCK-8, Cell Counting Kit-8; O.D, optical density; A549, human non-small cell lung cancer cells; MCF-7, human breast cancer cells; HepG2, human hepatocellular carcinoma cells; S180, murine sarcoma 180 cells; LLC, Lewis lung carcinoma cells; GA, 18 β -glycyrrhetic acid; GA-LDV, GA-Leu-Asp-Val.

GA-LDV Inhibits Cell Adhesion, Invasion and Migration

Fibronectin cell adhesion and transwell assays provide a fully quantitative method for evaluating cell adhesion, invasion and migration.²⁵ RGD peptides, known for their preferential binding to the α v β 3 integrin, significantly influence tumor cell adhesion, migration, and invasion.²⁶ Consequently, RGDS serves as a positive control in these experiments. As depicted in **Figure 2A** (first row) and **B**, the adhesion inhibition rates of GA and GA-LDV were 38.5% and 52.7%, respectively, significantly reduced the adhesion of LLC cells to the extracellular matrix (vs control group, $P < 0.05$). Notably, the anti-adhesion efficacy of GA-LDV was found to be equivalent to that of GA, indicating that the LDV modification did not compromise the inherent adhesive inhibitory capacity of the parent compound. Further analysis of the cells' invasive capabilities, as presented in **Figure 2A** (second rows) and **C**, both GA and GA-LDV significantly inhibited cell invasion (vs control group, $P < 0.01$). Importantly, the invasion inhibition rates of GA and GA-LDV were 27.5% and 37.9% ($P < 0.05$), respectively, revealing that GA-LDV had better anti-invasive activities than GA. As presented in **Figure 2A** (third rows) and **D**, both GA and GA-LDV significantly inhibited cell migration compared with the control group ($P < 0.01$). What's more, the migratory inhibition rates of GA and GA-LDV were 16.9% and 55.5% ($P < 0.05$), respectively, revealing that GA-LDV demonstrated better anti-migratory activities than GA, indicating that the LDV modification confers additional benefits.

GA-LDV Inhibits S180 Tumor Growth in vivo

The anti-tumor activity was evaluated using a S180 tumor-bearing mice model in vivo. The tumor weight in the Dox group, designated as the positive control, was significantly reduced compared to the control group, which implies that the modeling was successful. As illustrated in **Figure 3A**, the mean tumor weight in the GA and GA-LDV treatment group was notably lower than that of the control group ($P < 0.01$), suggesting the in vivo antitumor activity of GA-LDV was superior to that of GA in the S180 tumor mouse model ($P < 0.05$). Upon completion of the experiment, the body weights of the mice were assessed, as depicted in **Figure 3B**. It was observed that the body weights of the mice in the Dox-treated group were significantly diminished, which was likely attributed to the known side effects of Dox. In contrast, the body weights of mice in the GA and GA-LDV treatment groups remained unaffected, indicating that these treatments did not induce significant weight loss.

Hematoxylin and eosin (H&E) staining was performed to assess the histopathological effects of GA-LDV treatment on various organs of mice. The findings, as presented in **Figure 3C**, reveal that in contrast to the normal control mice, the cardiomyocytes in the GA-LDV treated group exhibited a well-organized and compact arrangement, with myocardial fibers maintaining their structural integrity. The brain cells displayed uniformity in their architectural and chromatic characteristics, devoid of any significant vacuolar degeneration. Furthermore, hepatic and splenic cells appeared morphologically intact, neatly aligned, and uniformly stained for cytoplasmic redness, with no notable enlargement of the cell nuclei. These histological observations indicate that GA-LDV treatment did not exert any substantial impact on the body weight or the morphological integrity of the organs in S180 tumor-bearing mice. The preservation of normal tissue architecture and the absence of severe pathological changes suggest that GA-LDV possesses a favorable safety profile, as it did not induce overt organ toxicity or significant weight loss in the treated animals.

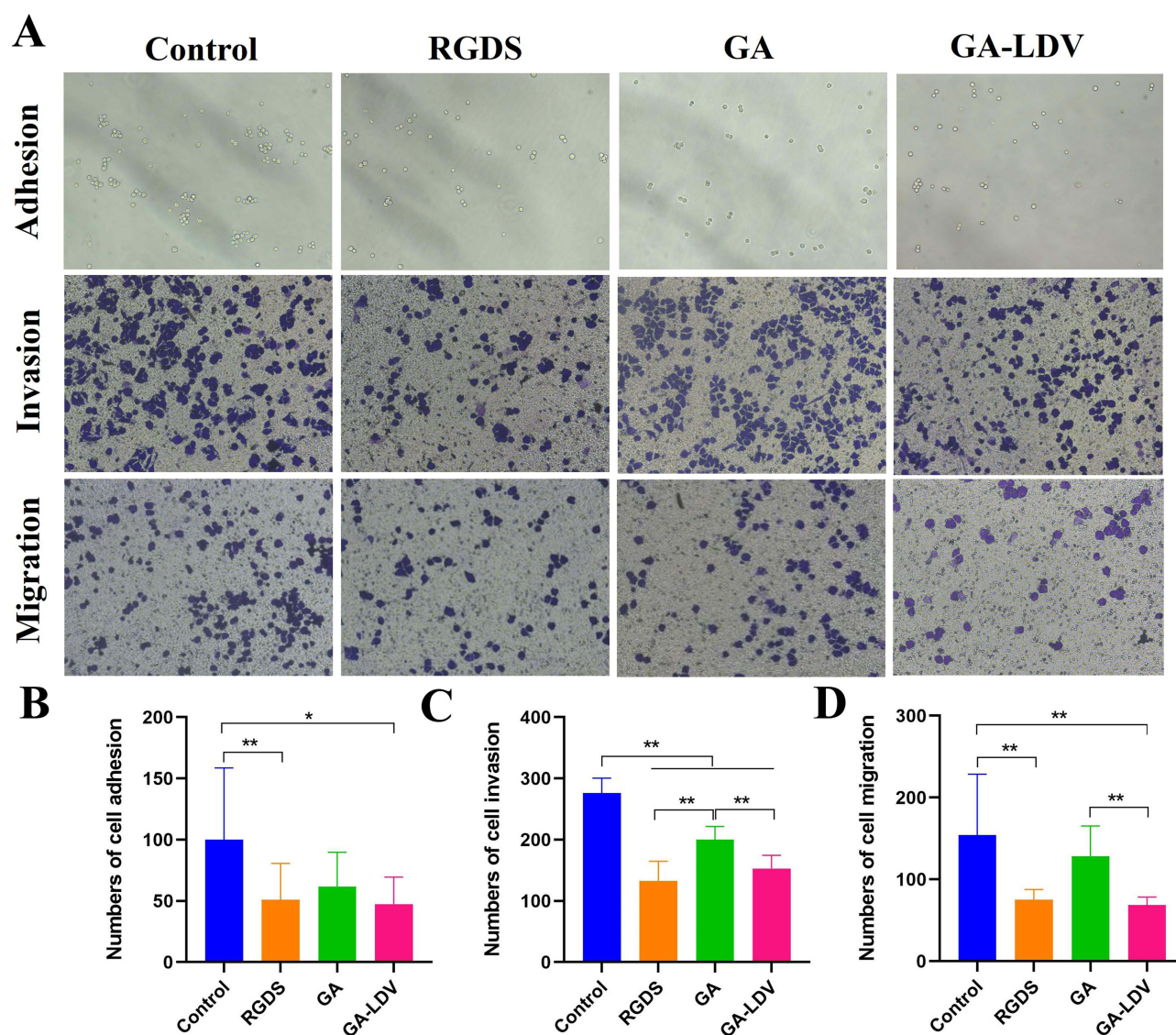


Figure 2 Effect of GA and GA-LDV on cell adhesion, invasion and migration in LLC cells. **(A)** Cells images treated with GA and GA-LDV. **(B)** The average number of adhesion cells was shown as a histogram. **(C)** The average number of invasive cells was shown as a histogram. **(D)** The average number of migratory cells was shown as a histogram. Data were expressed as mean \pm SD. * $P < 0.05$, ** $P < 0.01$.

Abbreviations: RGDS, Arg-Gly-Asp-Ser; GA, 18 β -glycyrrhetic acid; GA-LDV, GA-Leu-Asp-Val.

In the TUNEL staining assay, the intensity of the green fluorescence is directly proportional to the number of apoptotic cells present. As shown in **Figure 3D**, the sections from the vehicle-treated group predominantly displayed blue fluorescence with only a few sparse green dots, signifying that the majority of cells within the tumor tissue of this group remained active and non-apoptotic. In stark contrast, the tumor tissue sections from the GA-LDV group exhibited markedly enhanced green fluorescence ($P < 0.01$), indicative of a higher incidence (24-fold) of apoptosis among the tumor cells.

GA-LDV Effectively Inhibited the Metastasis of LLC Toward Lung in a Dose-Dependent Manner in vivo

The anti-metastasis activity of GA-LDV was evaluated on Lewis lung carcinoma (LLC) sarcoma implanted C57BL/6 mice, and the results were shown in **Figure 4**. **Figure 4A** showed representative lung fronts and backs of C57BL/6 mice bearing LLC sarcomas. As shown in **Figure 4B**, the mean numbers of lung metastatic nodules in mice in the control group and the positive

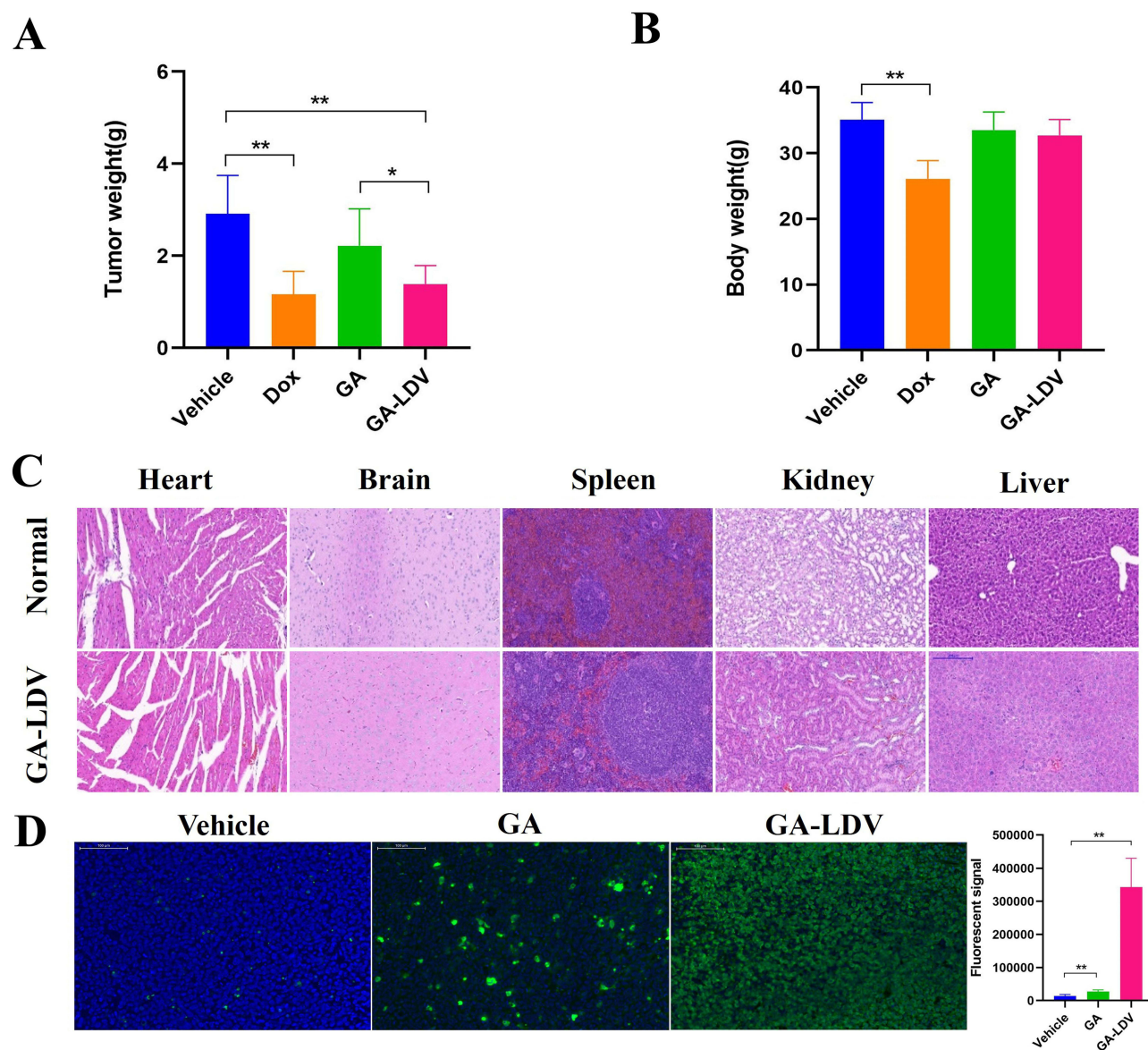


Figure 3 The anti-tumor effect of GA and GA-LDV on S180-bearing mice in vivo. **(A)** The tumor weight of S180-bearing mice. **(B)** The body weight of S180-bearing mice on the 15th day. **(C)** The different organs with H&E stain of S180-bearing mice treated by GA-LDV. **(D)** The TUNEL staining results of tumor tissue on S180-bearing mice. Data were expressed as mean \pm SD. * $P < 0.05$, ** $P < 0.01$.

Abbreviations: Dox, Doxorubicin; GA, 18 β -glycyrrhetic acid; GA-LDV, GA-Leu-Asp-Val.

group were 19.6 and 9.3 ($P < 0.01$), which implied that the modeling was successfully established. In the GA-LDV group at doses of 5 $\mu\text{mol/kg/d}$, 1 $\mu\text{mol/kg/d}$ and 0.2 $\mu\text{mol/kg/d}$, the mean numbers of lung metastatic nodules were 7.5 ($P < 0.01$, compared with the control group), 9.8 ($P < 0.05$, compared with the control group) and 14.5, respectively, significantly lower than that in the control group. The result indicated that the potential of GA-LDV to inhibit LLC tumor metastasis was dose-dependent. The lung sections with H&E stain of C57BL/6 mice treated by 5 $\mu\text{mol/kg/d}$ GA-LDV were showed in Figure 4E. Normal C57BL/6 mice were stained with clear alveolar structure and no obvious hyperplasia in the alveolar wall; in the vehicle group, the clusters of metastatic cancer cells (arrow) in the H&E staining of lungs were stained darker, with relatively dense cells and a large number of neutrophils infiltrated. The alveolar structure of C57BL/6 mice in the GA-LDV group was clear, and there was no obvious change compared with that in normal C57BL/6 mice, suggesting that GA-LDV had the activity of inhibiting the lung metastasis of LLC cells in C57BL/6 mice.

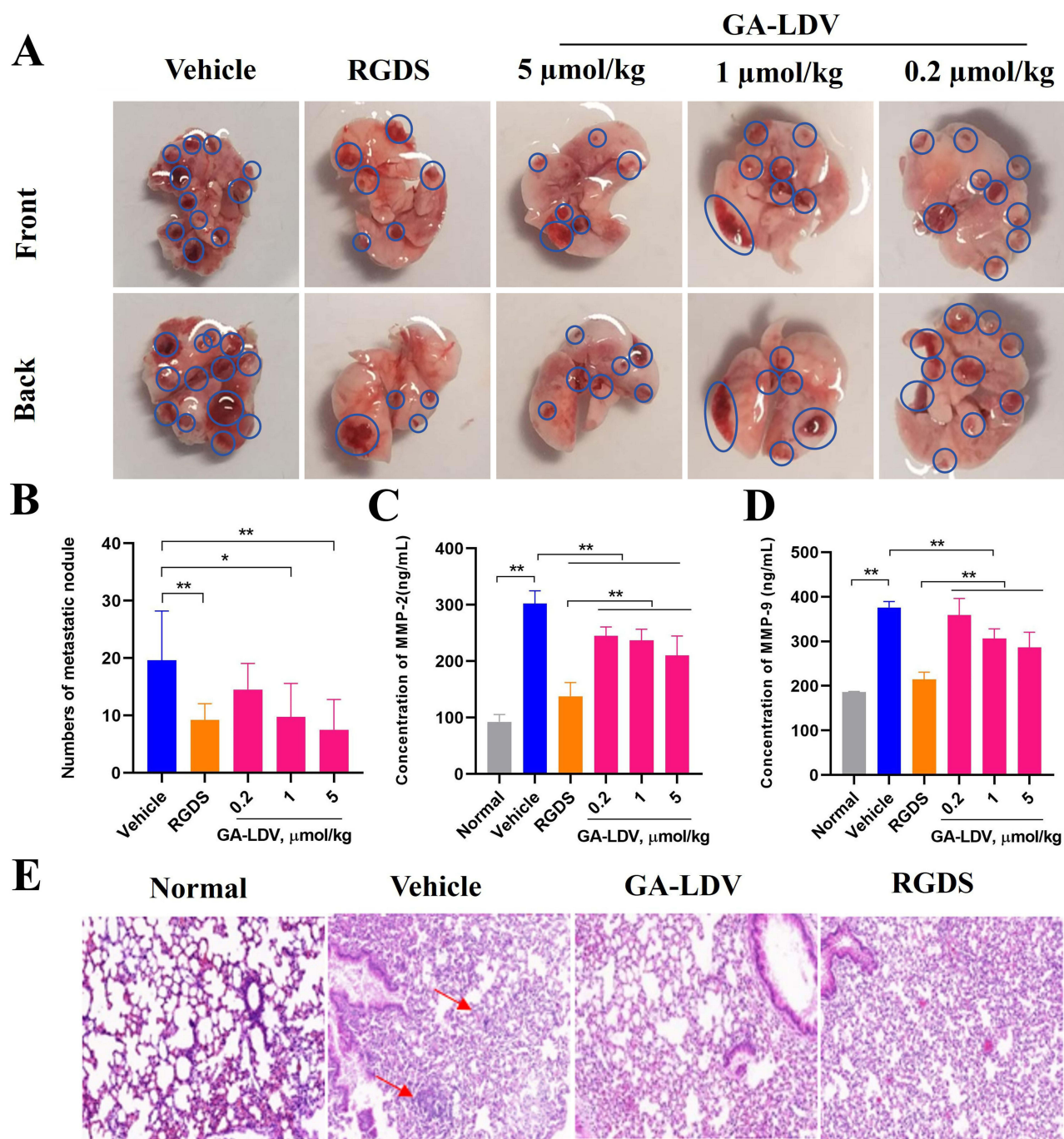


Figure 4 The anti-metastasis activity of GA-LDV on Lewis lung carcinoma (LLC) sarcoma implanted C57BL/6 mice in vivo. **(A)** Representative images of the lungs from C57BL/6 mice harboring LLC sarcomas treated with 5% CMC-Na (vehicle group), 20 $\mu\text{mol/kg/d}$ RGDS, and varying doses of GA-LDV (5, 1, and 0.2 $\mu\text{mol/kg/d}$) are presented. The number of metastatic nodules (indicated by red dots) on both the anterior and posterior aspects of the lungs correspond to the degree of lung cancer metastasis in the mice. **(B)** The number of lung metastasis nodules of LLC sarcoma-bearing C57BL/6 mice ($n=8$). **(C)** The level of MMP-2 in the serum of LLC sarcoma-bearing C57BL/6 mice. **(D)** The level of MMP-9 in the serum of LLC sarcoma-bearing C57BL/6 mice. **(E)** The lung sections with H&E stain of C57BL/6 mice. Arrow: the clusters of metastatic cancer cells. Data were expressed as mean \pm SD. * $P < 0.05$, ** $P < 0.01$.

Abbreviations: CMC-Na, carboxymethylcellulose-Na; RGDS, Arg-Gly-Asp-Ser; GA, 18 β -glycyrrhetic acid; GA-LDV, GA-Leu-Asp-Val; MMP-2, matrix metalloproteinase-2; MMP-9, matrix metalloproteinase-9.

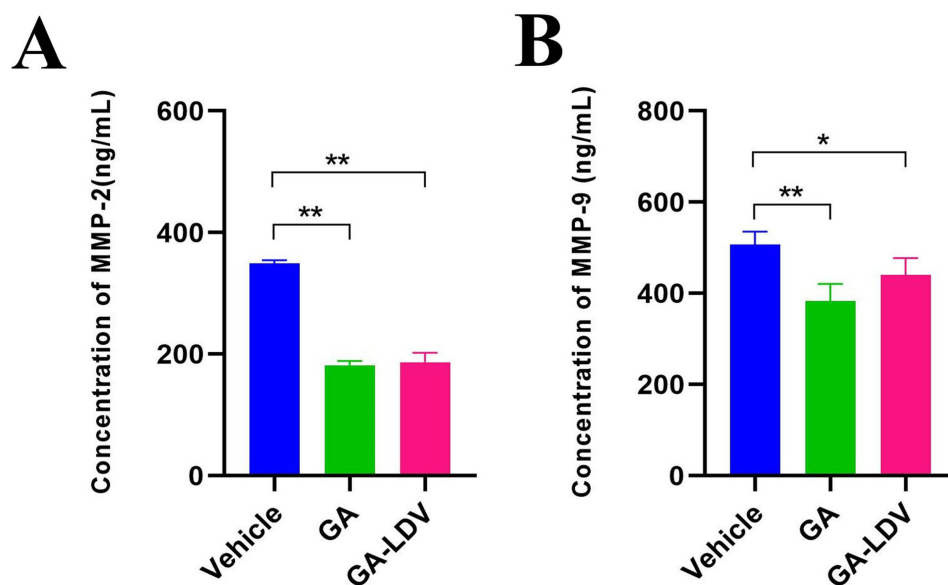


Figure 5 The level of MMP-2 (A) and MMP-9 (B) in the serum of S180-bearing mice. Data were expressed as mean \pm SD. * $P < 0.05$, ** $P < 0.01$. **Abbreviations:** GA, 18 β -glycyrrhetic acid; GA-LDV, GA-Leu-Asp-Val; MMP-2, matrix metalloproteinase-2; MMP-9, matrix metalloproteinase-9.

GA-LDV Inhibited the Expression of MMP-2 and MMP-9 in S180-Bearing Mice and LLC Sarcoma-Bearing C57BL/6 Mice

The serum MMP-2 and MMP-9 levels were detected using the ELISA assay kit. As shown in Figure 4C and D, the serum levels of MMP-2 and MMP-9 in the GA-LDV group were significantly lower than those in the control group at different doses of GA-LDV (5, 1, and 0.2 $\mu\text{mol/kg/d}$) ($P < 0.01$), suggesting that GA-LDV inhibited the expression of MMP-2 and MMP-9 in LLC sarcomas in C57BL/6 mice. As shown in Figure 5A and B, the serum MMP-2 and MMP-9 levels of GA and GA-LDV group were lower significantly than those in the control group ($P < 0.01$), indicating that GA and GA-LDV can both inhibit the expression of MMP-2 and MMP-9 in S180-bearing mice. These data suggested that the in vivo efficacy of GA-LDV in effectively inhibiting LLC metastasis to the lungs may be a result of its reduction of MMP-2 and MMP-9 levels in the serum of C57BL/6 mice implanted with LLC sarcomas.

Discussion

Glycyrrhizic acid (GA), one of the main active ingredients extracted from the traditional Chinese medicine *Glycyrrhiza glabra*, belongs to the triterpenoids class, and possesses a variety of pharmacological activities, such as anti-tumor and anti-tumor metastasis.²⁷ However, its lower anti-tumor activity limits its clinical application. Integrins have been recognized as compelling pharmacological targets for therapeutic agents designed to disrupt pivotal processes in cancer progression, including cell proliferation, survival, and migration.²⁸ The targeting of integrins to enhance the delivery of antitumor agents constitutes a novel and promising strategy.²⁹ Oligopeptide fragment Leu-Asp-Val (LDV), which is recognized for its high affinity to $\alpha 4\beta 1$ integrin, was strategic to augment the anti-cancer efficacy of GA. In this study, we synthesized a new compound GA-LDV by attaching the oligopeptide LDV to GA. The introduction of the LDV peptide significantly increased the solubility of GA-LDV by 4.13-fold relative to GA (161 $\mu\text{g/mL}$ vs 39 $\mu\text{g/mL}$). In vitro antiproliferative assay showed that GA-LDV exhibited antiproliferative activity comparable to GA and had no killing effect on normal cells. It was shown that GA significantly reduced the invasive and migratory activities of SGC-7901 cells and inhibited the activities of MMP-2 and 9 in a dose-dependent manner.²⁸ Our findings indicate that GA-LDV exhibited good in vitro anti-adhesion, anti-invasion and anti-migration activities, aligning with existing literature. In an in vivo S180 sarcoma model, the antitumor activity of GA-LDV (5 $\mu\text{mol/kg}$) was superior to that of GA (50.0% vs 24.0%, $P < 0.01$). The results of HE staining showed that GA-LDV had no significant effect on the organs, which indicated that GA-LDV has a good safety profile in vivo. In the Lewis mouse lung cancer metastasis model, 1 $\mu\text{mol/kg}$

and 5 $\mu\text{mol/kg}$ GA-LDV exhibited anti-tumor metastasis activity ($P < 0.01$), whereas 0.2 $\mu\text{mol/kg}$ GA-LDV did not inhibit tumor metastasis significantly, suggesting that GA-LDV has dose-dependent anti-tumor metastasis activity in vivo. HE staining results further confirmed that 5 $\mu\text{mol/kg}$ GA-LDV inhibited the metastasis of LLC tumor cells to lung tissues. Tunel staining results showed that tumor tissue sections in the GA-LDV group had strong green fluorescence, indicating that GA-LDV was able to induce apoptosis of tumor tissue cells in vivo. Several studies have shown that GA has an inhibitory effect on MMPs.^{14,30} We examined the expression levels of MMP-2 and MMP-9 in the serum of S180 mouse model and the Lewis mouse lung cancer metastasis model. The results showed that GA-LDV inhibited the expression of MMP-2 and MMP-9 in both models, which is consistent with the literature results.^{31,32} The oligopeptide sequence LDV served as a proof-of-concept to augment the anticancer efficacy of GA. These findings suggest that the conjugate GA-LDV may impede tumor growth and metastasis by downregulating the expression of MMP-2 and MMP-9, but more mechanisms and pathways need to be further explored.

Conclusion

In summary, we have designed and synthesized a novel GA derivative, GA-LDV, which exhibits enhanced water solubility, superior in vitro and in vivo antitumor efficacy, and notable antimetastatic activities, coupled with a favorable safety profile. The comprehensive study of GA-LDV offers valuable insights for the future development of antitumor drugs and their clinical applications.

Funding

This study was funded by Significant new drugs creation “Five-Year plan” special science and Technology Major (2018ZX097201003), NSFC (81703332) and Scientific Research Common Program of Beijing Municipal Commission of Education (KM201810025010).

Disclosure

The authors report no conflicts of interest in this work.

References

- Ganesh K, Massagué J. Targeting metastatic cancer. *Nat Med.* 2021;27(1):34–44. doi:10.1038/s41591-020-01195-4
- Gerstberger S, Jiang Q, Ganesh K. Metastasis. *Cell.* 2023;186(8):1564–1579. doi:10.1016/j.cell.2023.03.003
- Hebert JD, Neal JW, Winslow MM. Dissecting metastasis using preclinical models and methods. *Nat Rev Cancer.* 2023;23(6):391–407. doi:10.1038/s41568-023-00568-4
- de Visser KE, Joyce JA. The evolving tumor microenvironment: from cancer initiation to metastatic outgrowth. *Cancer Cell.* 2023;41(3):374–403. doi:10.1016/j.ccell.2023.02.016
- Conlon GA, Murray GI. Recent advances in understanding the roles of matrix metalloproteinases in tumour invasion and metastasis. *J Pathol.* 2019;247(5):629–640. doi:10.1002/path.5225
- Abdel-Hamid NM, Abass SA. Matrix metalloproteinase contribution in management of cancer proliferation, metastasis and drug targeting. *Mol Biol Rep.* 2021;48(9):6525–6538. doi:10.1007/s11033-021-06635-z
- Raab-Westphal S, Marshall JF, Goodman SL. Integrins as therapeutic targets: successes and cancers. *Cancers.* 2017;9(9):110. doi:10.3390/cancers9090110
- Chen JR, Zhao JT, Xie ZZ. Integrin-mediated cancer progression as a specific target in clinical therapy. *Biomed Pharmacother.* 2022;155:113745. doi:10.1016/j.biopha.2022.113745
- Jin H, Varner J. Integrins: roles in cancer development and as treatment targets. *Br J Cancer.* 2004;90(3):561–565. doi:10.1038/sj.bjc.6601576
- Garmy-Susini B, Avraamides CJ, Schmid MC, et al. Integrin $\alpha 4 \beta 1$ signaling is required for lymphangiogenesis and tumor metastasis. *Cancer Res.* 2010;70(8):3042–3051. doi:10.1158/0008-5472.CAN-09-3761
- Anselmi M, Baiula M, Spampinato S, Artali R, He T, Gentilucci L. Design and pharmacological characterization of $\alpha 4 \beta 1$ integrin cyclopeptide agonists: computational investigation of ligand determinants for agonism versus antagonism. *J Med Chem.* 2023;66(7):5021–5040. doi:10.1021/acs.jmedchem.2c02098
- Gérard E, Meulle A, Feron O, Marchand-Brynaert J. Diaryl urea LDV peptidomimetics as $\alpha 4 \beta 1$ integrin antagonists: synthesis, adhesion inhibition and toxicity evaluation on CCRF-CEM cell line. *MedChemComm.* 2012;3:199–212. doi:10.1039/C1MD00229E
- He T, Giacomini D, Tolomelli A, Baiula M, Gentilucci L. Conjecturing about small-molecule agonists and antagonists of $\alpha 4 \beta 1$ integrin: from mechanistic insight to potential therapeutic applications. *Biomedicines.* 2024;12(2):316. doi:10.3390/biomedicines12020316
- Cai H, Chen X, Zhang J, Wang J. 18β -glycyrrhetic acid inhibits migration and invasion of human gastric cancer cells via the ROS/PKC- α /ERK pathway. *J Nat Med.* 2018;72(1):252–259. doi:10.1007/s11418-017-1145-y
- Wang S, Shen Y, Qiu R, Chen Z, Chen Z, Chen W. 18β -glycyrrhetic acid exhibits potent antitumor effects against colorectal cancer via inhibition of cell proliferation and migration. *Int J Oncol.* 2017;51(2):615–624. doi:10.3892/ijo.2017.4059

16. Ma X, Sun Z, Chen H, et al. 18 β -glycyrrhetic acid suppresses Lewis lung cancer growth through protecting immune cells from ferroptosis. *Cancer Chemother Pharmacol.* 2024;93(6):575–585. doi:10.1007/s00280-024-04639-7
17. Li WX, Lu YF, Wang F, et al. Application of 18 β -glycyrrhetic acid in the structural modification of natural products: a review. *Mol Divers.* 2024;29:739–781. doi:10.1007/s11030-024-10864-2
18. Quan W, Kong S, Ouyang Q, et al. Use of 18 β -glycyrrhetic acid nanocrystals to enhance anti-inflammatory activity by improving topical delivery. *Colloids Surf B Biointerfaces.* 2021;205:111791. doi:10.1016/j.colsurfb.2021.111791
19. Cai Y, Xu Y, Chan HF, Fang X, He C, Chen M. Glycyrrhetic acid mediated drug delivery carriers for hepatocellular carcinoma therapy. *Mol Pharm.* 2016;13(3):699–709. doi:10.1021/acs.molpharmaceut.5b00677
20. Kerns EH, Di L, Carter GT. In vitro solubility assays in drug discovery. *Curr Drug Metab.* 2008;9(9):879–885. doi:10.2174/138920008786485100
21. Cai L, Qin X, Xu Z, et al. Comparison of cytotoxicity evaluation of anticancer drugs between real-time cell analysis and CCK-8 method. *ACS Omega.* 2019;4(7):12036–12042. doi:10.1021/acsomega.9b01142
22. Justus CR, Marie MA, Sanderlin EJ, Yang LV. Transwell in vitro cell migration and invasion assays. *Methods mol Biol.* 2023;2644:349–359. doi:10.1007/978-1-0716-3052-5_22
23. Zhang X, Jiang L, Li Y, et al. Discovery of novel benzylquinazoline molecules as p97/VCP inhibitors. *Front Pharmacol.* 2023;14:1209060. doi:10.3389/fphar.2023.1209060
24. Zhang X, Zhang J, Liu W, et al. Exploring the action of RGDV-gemcitabine on tumor metastasis, tumor growth and possible action pathway. *Sci Rep.* 2020;10(1):15729. doi:10.1038/s41598-020-72824-8
25. Pijuan J, Barceló C, Moreno DF, et al. In vitro cell migration, invasion, and adhesion assays: from cell imaging to data analysis. *Front Cell Dev Biol.* 2019;7:107. doi:10.3389/fcell.2019.00107
26. Danhier F, Le Breton A, Pr at V. RGD-based strategies to target alpha(v) beta(3) integrin in cancer therapy and diagnosis. *Mol Pharm.* 2012;9(11):2961–2973. doi:10.1021/mp3002733
27. Hasan MK, Ara I, Mondal MSA, Kabir Y. Phytochemistry, pharmacological activity, and potential health benefits of *Glycyrrhiza glabra*. *Heliyon.* 2021;7(6):e07240. doi:10.1016/j.heliyon.2021.e07240
28. Pang X, He X, Qiu Z, et al. Targeting integrin pathways: mechanisms and advances in therapy. *Signal Transduct Target Ther.* 2023;8(1):1. doi:10.1038/s41392-022-01259-6
29. Li M, Wang Y, Li M, Wu X, Setrerrahmane S, Xu H. Integrins as attractive targets for cancer therapeutics. *Acta Pharm Sin B.* 2021;11(9):2726–2737. doi:10.1016/j.apsb.2021.01.004
30. Rehman MU, Farooq A, Ali R, et al. Preclinical evidence for the pharmacological actions of glycyrrhizic acid: a comprehensive review. *Curr Drug Metab.* 2020;21(6):436–465. doi:10.2174/1389200221666200620204914
31. Wang Y, Wang L, Luo R, et al. Glycyrrhizic acid against *Mycoplasma gallisepticum*-induced inflammation and apoptosis through suppressing the MAPK pathway in chickens. *J Agric Food Chem.* 2022;70(6):1996–2009. doi:10.1021/acs.jafc.1c07848
32. Wang XF, Zhou QM, Lu YY, Zhang H, Huang S, Su SB. Glycyrrhetic acid potently suppresses breast cancer invasion and metastasis by impairing the p38 MAPK-AP1 signaling axis. *Expert Opin Ther Targets.* 2015;19(5):577–587. doi:10.1517/14728222.2015.1012156

Drug Design, Development and Therapy

Publish your work in this journal

Drug Design, Development and Therapy is an international, peer-reviewed open-access journal that spans the spectrum of drug design and development through to clinical applications. Clinical outcomes, patient safety, and programs for the development and effective, safe, and sustained use of medicines are a feature of the journal, which has also been accepted for indexing on PubMed Central. The manuscript management system is completely online and includes a very quick and fair peer-review system, which is all easy to use. Visit <http://www.dovepress.com/testimonials.php> to read real quotes from published authors.

Submit your manuscript here: <https://www.dovepress.com/drug-design-development-and-therapy-journal>

Dovepress
Taylor & Francis Group